University of Utah
UNDERGRADUATE RESEARCH JOURNAL

THE HIV-PROTECTIVE BYSTANDER EFFECT IN MACROPHAGES IS VIRAL GLYCOPROTEIN DEPENDENT AND LIKELY CONFERRED VIA UPREGULATION OF ISG IFITM3

Nathaniel Thomas, Vicente Planelles, Elizabeth Williams
Department of Pathology

ABSTRACT

During an immune response against a specific antigen, often during viral infections, T cells not specific to the antigen can be activated, a phenomenon known as bystander response. The "bystander response" has been studied extensively in T cells, but when examined for macrophages through the lens of HIV, it has a different outcome and is referred to as the "bystander effect". The bystander effect is seen when macrophages are exposed to a primary infection with HIV and results in increased protection of these macrophages to a secondary infection with HIV. Based on earlier experiments in the Planelles Lab, we hypothesized that the viral envelope is responsible for the bystander effect. We tested this hypothesis by generating HIV viruses pseudotyped with unique envelopes and subjecting human macrophages with primary and secondary HIV infections to induce the bystander effect. The number of cells infected by the secondary infection was measured using fluorescent markers to determine the level of protection offered by each unique envelope. Our experiments showed a bystander effect protection level of 99% or greater with the envelopes supporting our hypothesis. The exact cause of the bystander effect is now being investigated to shed more light on this phenomenon.

INTRODUCTION

History of HIV: epidemic, identification, clinical significance, and viral life cycle

Human immunodeficiency virus (HIV) was identified in the early 1980's as being responsible for inducing acquired immunodeficiency syndrome (AIDS); the lethal wasting sickness that causes depleted levels of CD4+ T-cells and resulted in patients becoming susceptible to opportunistic infections (Damtie et al., 2013). Patients suffering from AIDS experienced varying symptoms of pneumonia, dysphagia, diarrhea, blindness, fever, among other symptoms depending on the severity of infection (Lloyd, 1996). The HIV/AIDS epidemic devastated both civil order and economic growth (Gayle & Hill, 2001). Communities worldwide were hurt by this disease, primarily those living in developing countries (Gayle & Hill, 2001). To combat the epidemic, a new form of treatment, in the form of antiretroviral therapy (ART) was created. While ART was groundbreaking, some people had complications including, but not limited to: nausea, diarrhea, fatigue, headache, lactic acidosis, osteoporosis, hepatotoxicity, hyperglycemia, etc. throughout their treatment (Montessori et al., 2004).

HIV is a retrovirus that infects CD4+ T cells, monocytes, and other macrophage-lineage cells in vivo (Wong et al., 2019). This paper focuses on HIV infection in monocyte derived macrophages (MDMs). To productively infect MDMs, the HIV virus binds to the CD4 receptor and the CCR5 co-receptor on the cell surface (Fig. 1). The viral envelope will fuse with the MDM cell surface membrane allowing the HIV core, or capsid (which encapsulates the viral RNA genome) to enter the cell cytoplasm (Fig. 2). After cellular entry, the capsid is trafficked to the nuclear membrane, where it degrades in a process called uncoating and undergoes nuclear entry (Fig. 1). HIV has a single stranded RNA genome and requires reverse transcription into pro-viral DNA before it can integrate into the host cell genome. Once integrated, the virus can complete its life cycle by co-opting the host cell machinery to transcribe the viral RNA, for transportation of the RNA into the cytoplasm, translation, and assembly into immature virions that bud from the cell surface prior to maturing into fully infectious virions (Fig. 1).

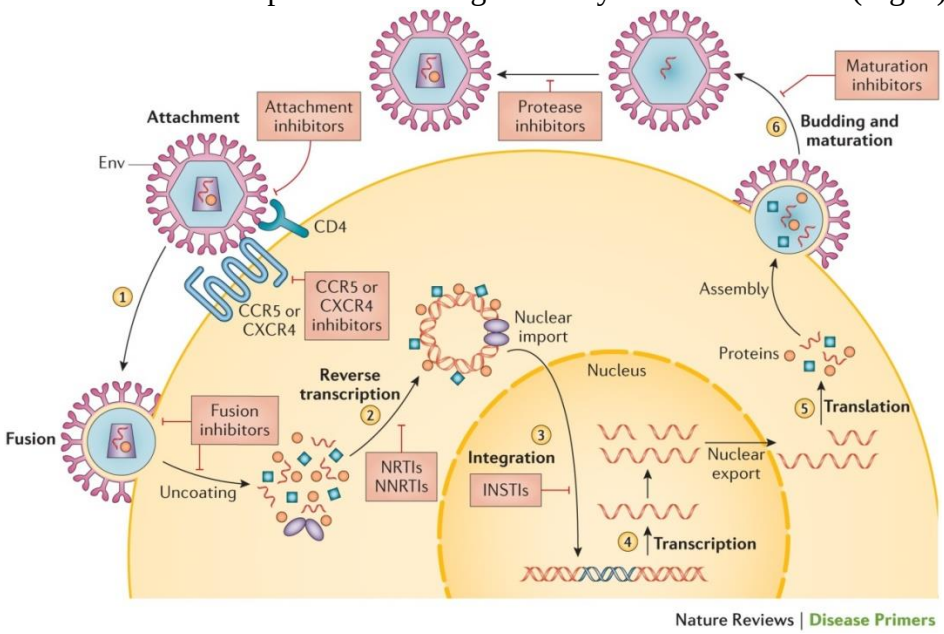

Fig. 1. A complete depiction of the HIV life cycle. The most notable steps of this process are: attachment, fusion, uncoating, reverse transcription, integration, transcription, translation, and budding leading to maturation. (Credit to: Deeks et al., 2015).

Since the initial development of ART, many new treatment options have arisen. There are now seven classes of ART which inhibit multiple aspects of the viral life cycle including viral entry, reverse transcription, integration, assembly and budding (Clercq, 2010). Currently, most people living with HIV (PLWH) in the industrialized world take only one or two pills a day that contain combination ART (cART). cART is extremely effective at inhibiting progression of HIV infection into AIDS, allowing many PLWH to live long and healthy lives.

Many advances have been made in the treatment of HIV, one of the more recent being the clinical use of cART as pre-exposure prophylaxis (PrEP) for individuals at high risk of contracting HIV (Leech et al., 2020). At almost 40 years since the identification of HIV, there is still no preventative vaccine, and it is estimated that around 37.9 million people are currently infected with HIV worldwide, with approximately 1.7 million new infections still occurring each year (Mahy et al., 2019).

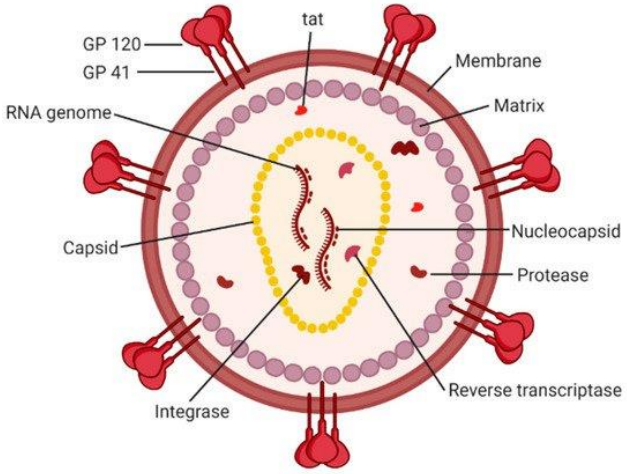

Fig. 2. A diagram of the HIV-1 virion. Viral envelope proteins are embedded in the host derived phospholipid envelope while the capsid houses the viral RNA genome. (Credit to: Eric Rossi et al., 2021).

Gene Therapy and Viral Restriction Factors

The development of new treatments for diseases has been a central goal of biological research for decades. Innovative techniques to create treatments are necessary for progress, and different techniques of gene therapy have evolved over the years. Early gene therapy revolved around the usage of recombinant DNA (Wirth et al., 2013). Research on performing gene therapy in the most seamless way became a top priority and was used more often in a clinical setting.

As research continued, some limitations for the use of retroviral vector systems were discovered. Some of the most problematic limitations were that the vectors were unable to infect non-dividing or terminally differentiated cells (Buchschacher & Wong-Staal, 2000). Researchers have spent years trying to develop a workaround for these vectors, but with little success. Eventually, it was discovered that these retroviral vectors were able to enter non-dividing cells, but that the nuclear envelope of non-dividing cells was protecting the cell nucleus, preventing nuclear entry (Buchschacher & Wong-Staal, 2000). If replication was unable to occur, a “proper” infection would be impossible in these cells, meaning only actively dividing cells could be infected and allow for a complete replication cycle. The solution to this problem came from scientists with a completely different perspective.

The solution emerged from studies that were trying to understand HIV and its replication cycle. Scientists began to hypothesize that HIV could be used as a vector instead of using other retroviruses. This led to one of the most notable contributions that stemmed from HIV research- the discovery that HIV and other lentiviruses could be used as vectors for gene therapy (Pluta & M. Kacprzak, 2009). The new approach to conducting gene therapy was met with some resistance until it was discovered that HIV was able to successfully infect non-dividing and terminally differentiated cells (Pluta & M. Kacprzak, 2009). Using lentiviruses as vectors for gene therapy works well because the vectors can integrate directly into the host DNA (Pluta & M. Kacprzak, 2009). Both the ability to infect non-dividing cells and the precise targeting of sections of DNA revolutionized gene therapy techniques, which is why lentiviruses are still used experimentally today.

The last forty years of HIV research has led to many scientific breakthroughs across many branches of human biology. The identification of novel host viral restriction factors are some of the most notable. This class of proteins directly functions to inhibit HIV (and other RNA and DNA viruses) infection at various stages of the viral life cycle. There are a total of nine known restriction factors that target HIV specifically, and the four most well documented are:

apolipoprotein B mRNA editing enzyme, catalytic subunit 3G (APOBEC3G), Tripartite motif-containing protein 5 (TRIM5α), sterile alpha motif and histidine-aspartic acid domain containing protein 1 (SAMHD1), and Tetherin (Colomer-Lluch et al., 2018). APOBEC3G can be encapsidated into budding virions and by catalyzing deamination; it causes high levels of hypermutations in proviral DNA, leading to many premature STOP codons (Colomer-Lluch et al., 2018). TRIM5α has many powerful antiviral activities, and one reason for this is because it directly binds to the incoming retroviral capsid, driving the premature uncoating of HIV-1, which impairs reverse transcription from occurring (Colomer-Lluch et al., 2018). Tetherin has a unique topology that allows it to anchor budding viral particles on the surface of infected cells, preventing the release of HIV-1 virions (Colomer-Lluch et al., 2018).

The restriction factor most relevant to this project is SAMHD1, a deoxynucleotide triphosphate (dNTP) triphosphohydralase that cleaves dNTPs into their nucleotide base and inorganic phosphate components (Cribier et. al, 2013). The normal function of SAMHD1 is cell cycle regulated and results in a smaller number of dNTPs present within dividing cells when they are not undergoing replication (Coggins et. al, 2020). When preparing for replication, SAMHD1 is deactivated through phosphorylation, causing the number of dNTPs to increase. In macrophages, which are terminally differentiated, SAMHD1 is usually in its active, unphosphorylated state, where it degrades dNTPs, which has the added benefit of keeping the cellular levels of dNTPs too low to support successful reverse transcription of RNA viruses such as HIV, resulting in its identification as a restriction factor (Cribier et. al, 2013)

Although not among the four most well documented restriction factors, the interferon-induced transmembrane (IFITM) proteins are also known to protect cells from various viral infections, and IFITM3 specifically tends to reduce both virus fusion and cell-to-cell spread of HIV (Compton et. al, 2016). IFITM1, IFITM2, and IFITM3 have been known to protect cells from many types of viral infections, studying these proteins and how they interact with HIV will help elucidate one mechanism of host cell defense against HIV. The interactions between the viral restriction factors IFITM3 and SAMHD1 also relate to gene therapy because SAMHD1 also restricts the infection of MDMs by other DNA and RNA viruses, including some lentiviruses such as equine infectious anemia virus (EIAV) and feline immunodeficiency virus (FIV) (Coggins et. al, 2020).

Pseudotypes using amphotropic murine leukemia virus (AMLV) and lymphocytic choriomeningitis virus (LCMV) envelopes

Studying the behaviour of retroviral vectors can be difficult due to retroviral instability, which is why pseudotypes were developed to bypass this problem (Miletic et al., 1999). Pseudotyped viruses (Fig. 3) are viral particles that have the structural and enzymatic core from one virus, and the envelope glycoprotein of different virus (Bentley et al., 2015). This began with the development of pseudotyped viruses of AMLV that allowed for increased levels of retroviral stability, at a much faster rate compared to before (Landau & Littman, 1992). Building off this achievement, LCMV pseuotyped viruses were developed and also offered high levels of retroviral stability (Landau & Littman 1992). Both of these developments in AMLV and LCMV pseudotyped viruses were important as they opened the doors for improved vector stability and transduction efficiency (Miletic et al., 1999).

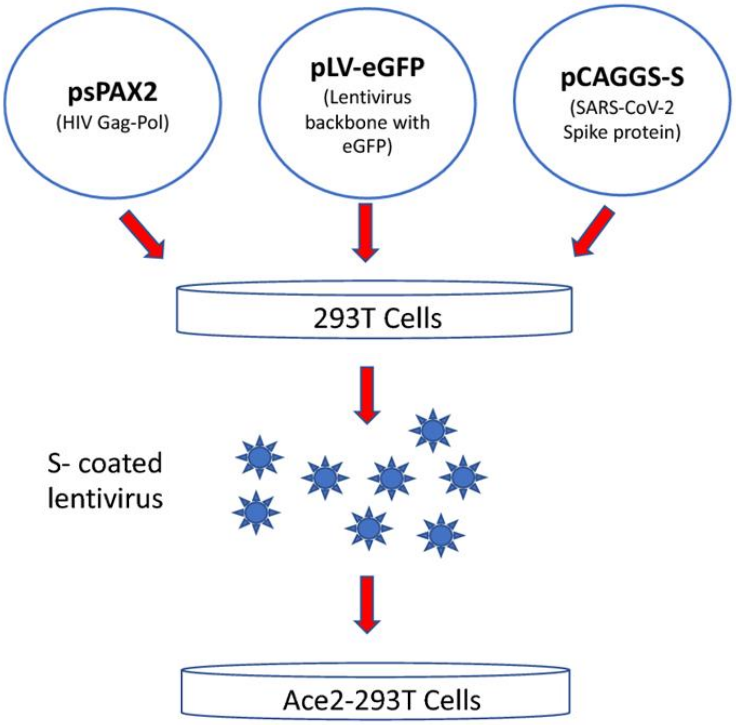

Fig. 3. An example of a pseudotyped virus using an HIV Gag-Pol, lentivirus backbone, and a SARS-CoV-2 spike protein. These components can be combined to form replication defective lentivirus particles pseudotyped with the SARS CoV-2 spike protein. (Credit to: Tandon et al., 2020).

Experimental Background

The concept of "bystander activation" in immunology has been interpreted as the stronger response of T cells after being primed from an initial infection (Kim & Shin, 2019). An example of bystander activation, in this context, can be seen after a naïve T cell has a virus specific response, which then results in the formation of a virus-specific memory T cell (Fig. 4). Then, when a similar (or same) virus infects the host at some point after the initial infection, the "bystander activation" of the memory T cells will result in a quick and more effective response against the secondary infection (Kim & Shin, 2019).

With respect to T cell infection by HIV, the classical definition of "bystander response" is not applicable because the immune response damages the host (Kim & Shin, 2019). Rather than protecting the host, the response from the bystander cells results in either bystander apoptosis or bystander pyroptosis (Garg & Joshi, 2017). It is believed that bystander cell degradation causes the death of CD4 T cells, ultimately leading to the development of AIDS (Garg & Joshi, 2017).

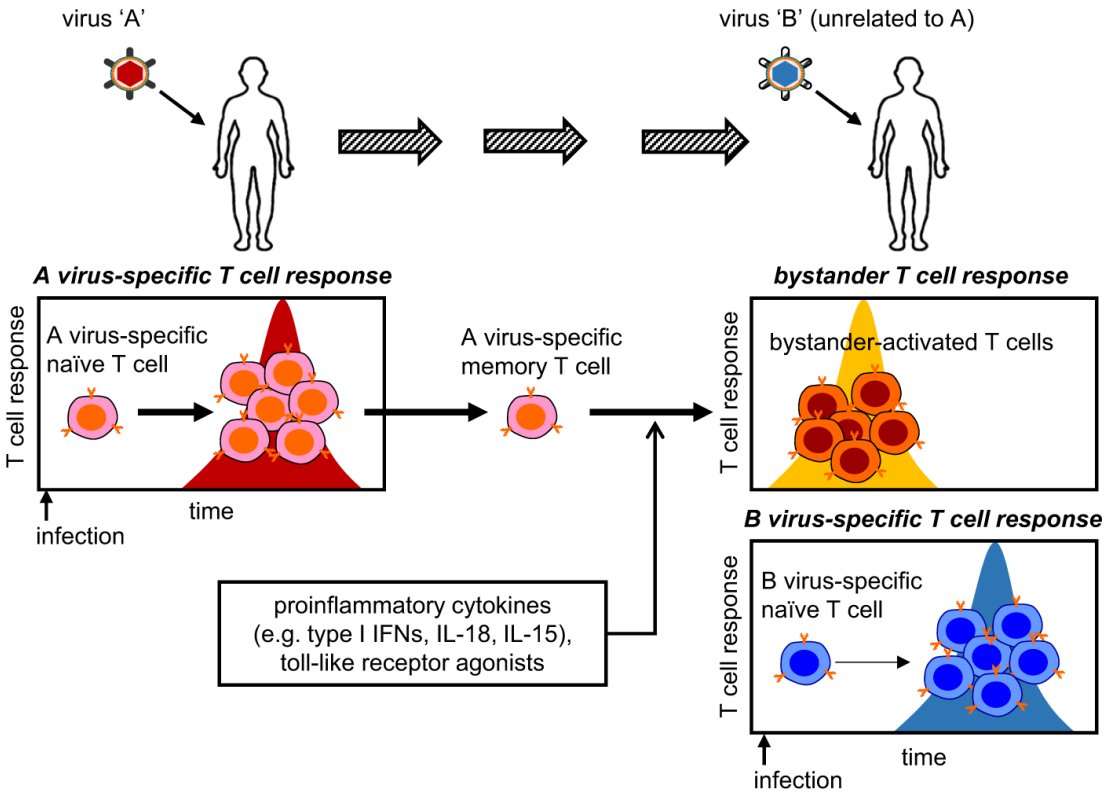

Fig. 4. A depiction of the bystander activated response seen in T cells. After an initial infection from virus 'A', virus-specific memory T cells are created, that allow for a stronger and earlier response to a secondary infection of a similar yet unrelated virus 'B'. (Credit to: Kim & Shin, 2019).

The Planelles Lab, where I have conducted my honors thesis research, has been attempting to define what the "bystander effect" in response to HIV infection looks like in primary human monocyte derived macrophages (MDMs). This area of research evolved from a series of observations:

1. HIV infection of MDMs dephosphorylates SAMHD1 (Fig. 5).
2. Utilization of a molecular tool that replaces the HIV envelope protein with the envelope protein from the Vesicular Stomatitis Virus (VSV); rendering the virus replication deficient and thus safer and easier to work with in the laboratory (DePolo et al., 2000) often results in a greater degree of SAMHD1 dephosphorylation in response to infection (Fig. 5).

These observations lead to the following question(s): If HIV infection of MDMs dephosphorylates SAMHD1 and creates a cellular environment that is protected from infection, would it be harder to infect them with a second HIV virus? In other words, is the initial HIV infection causing a protective "bystander effect" that will protect the uninfected cells from a secondary HIV infection? And, does the VSV envelope induce a stronger IFITM3 response, and thus a greater dephosphorylation of SAMHD1 than the HIV envelope?

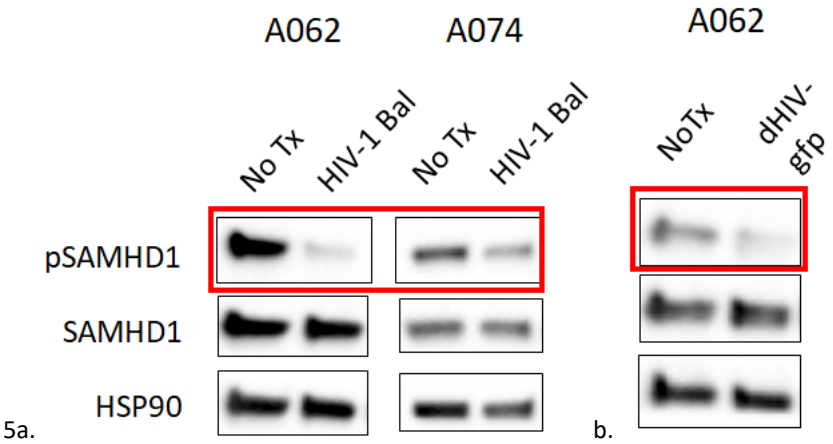

Fig. 5. Data from the Planelles Lab that showed HIV-1 infection of MDMs will dephosphorylate SAMHD1, both when using a replication competent virus (4a.), and when using one that is pseudotyped with VSVg (4b.). The A062 an A074 are in reference to different blood donors. No Tx is in reference to no treatment, HIV-1 Bal is referencing the replication competent virus, and dHIV-gfp is referencing the virus pseudotyped with VSVg. (Credit to Elizabeth Williams, Unpublished data).

METHODS

Bacterial Transformation

50 µl of stbl3 competent *E. coli* cells (used as they have a lower likelihood of recombination) were thawed on ice for five minutes. 1-5 µl of viral plasmid was added to stbl3 competent cells and mixed gently (1 µl added if the plasmid concentration was more than 1000 ng/µl and 5 µl was added if the concentration was less than 100 ng/µl). Cells with plasmid were incubated on ice for 15 minutes and heat shocked for 30 seconds by placing them at 42°C, and then put them back on ice for two minutes. 1 ml of Luria broth (LB) with no antibiotics was added to the cells and placed in a shaking incubator for 40 minutes at 37°C. Various volumes of cells were plated on LB agar plates supplemented with ampicillin to select for plasmid uptake. Plates were incubated at 37°C overnight to allow for bacterial growth and moved to 4°C the following morning.

Pre-Maxi Prep with Aseptic Technique

The plated colonies of *E. coli* were removed from the fridge to determine which singular colonies could be picked from each plate. Multiple 2800 ml Erlenmeyer flasks were gathered and labeled with the individual plasmid names. A Bunsen burner was lit and the lip of the LB broth bottle was passed through the flame to maintain sterility. 250 ml of LB were measured with a sterile graduated cylinder while staying below the flame for sterilization. The measured LB from the graduated cylinder was poured into the flask and immediately covered with aluminum foil, while keeping it under the flame. A small pipette tip was used to pick out the single colony marked earlier and was quickly put into the flask which was covered immediately.

Maxi Prep

Plasmid DNA isolation was conducted using a Qiagen Plasmid Maxi Kit (100) catalogue number 12165. The culture containing the grown *E. coli* colony with LB was poured into a sterile bottle and centrifuged for 10 minutes at 4300 rpm, 4°C. The supernatant was poured out and 12 ml of resuspension/RNAse A solution was used to resuspend the bacterial pellet. This mixture was transferred to a 50 ml falcon tube where 12 ml of lysis solution was added and

mixed by inverting the tube 6 times. While letting the mixture sit for 5 minutes until it was clear and viscous (to ensure all bacterial cells lyse), a filter for the Maxi prep was prepared. The plunger of a large plastic syringe was removed and the syringe was placed upright in a large test tube rack. 12 ml of neutralization solution was added to the mixture in the falcon tube and inverted 6 times to mix them both together. After a white aggregate formed in the falcon tube, 9 ml of binding solution was added, the tube was inverted twice, and the mixture was poured into the syringe filter.

While letting the mixture sit in the filter for 5 minutes so the white aggregate would float to the top of the liquid, a binding column was placed directly into the hole on a vacuum apparatus (the vacuum was connected to the vacuum valve on the bench and a rubber stopper was put on the other end). 12 ml of column prep solution was added and passed through the newly created vacuum column. The syringe filter was used to filter the cellular debris from the remaining liquid into a clean 50 ml falcon tube, and this mixture was poured into the vacuum column. 12 ml of wash solution was passed through the vacuum column which remained attached to the vacuum for 10 minutes to dry.

The column was moved to a clean 50 ml falcon tube, and without touching the side of the column, a pipette was used to add 3 ml of elution solution evenly over the column. While the mixture spun down for 5 minutes at 4300 rpm, 4°C, 170 µl of 5 M NaCl were taken and combined with 6 ml of 100% cold EtOH. This was added to the mixture after it has been spun down without removing the elutant, and the new mixture was spun down for 30 minutes at 4300 rpm, 4°C. The supernatant layer was decanted and the pellet of DNA in the tube (may not be visible but was present) was washed with 10 ml of cold 70% EtOH and the mixture was spun for 30 minutes at 4300 rpm, 4°C. The supernatant layer was decanted again and the tube was inverted over a piece of paper towel and ambient air entered the tube for an hour in order to let the pellet dry (time varied, didn't proceed until all the ethanol evaporated and the pellet was completely dry). The pellets were resuspended in water and quantified using a NanoDrop (300 µl of water was used to resuspend if the pellets were visible and 100 µl of water were used to resuspend the pellets if they weren't visible).

Thawing Frozen Cell Lines

The process of splitting human embryonic kidney 293FT (HEK-293FT) cells began with making the appropriate media using a bead bath to warm/thaw a sterile 500 ml bottle of Dulbecco's Modified Eagle Medium (DMEM), a pre-aliquoted 5 ml frozen tube of L-glutamine (L-glut), and a pre-aliquoted 50 ml tube of frozen Fetal Bovine Serum (FBS). After the FBS and L-glut completely thawed, their tubes and the sterile bottle of DMEM were cleaned with EtOH and placed in the tissue culture hood. L-glut and FBS were added to the DMEM and shaken well to create the media.

10 ml of pre-warmed media was placed in a 15 ml falcon tube and a pipette was used to transfer 200 µl of media to thaw the tube of HEK-293FT cells. To thaw the cells faster and give them an appropriate media to grow in, they were stirred and media was continuously added and removed by placing the mixed media that had thawed HEK-293FT cells back into the 15 ml falcon tube. This tube was centrifuged for 5 minutes at 1500 rpm, 4°C, and afterwards, the media from the tube was aspirated, leaving a pellet of cells at the bottom, which was resuspended in 10 ml of media. The 10 ml of cells mixed with media was added to a T-175 cell culture flask with an additional 10 ml of pure media, resulting in 20 ml of media in the flask. The flask was placed horizontally and gently shaken to evenly disperse the cells across the internal surface of the flask in a 37°C incubator for 3-5 days (time dependent on cell growth rate).

Splitting Cell Lines

When cell confluence was 60-70% or higher, they were split in a standardized process. The media was aspirated out of the cell culture flask and 6 ml of phosphate buffer saline (PBS) was added on the front facing side of the flask (the side that does not have the cells attached to it). The flask was laid flat on the cell facing side to allow the PBS to spread across the entire surface for around 30 seconds, after which it was aspirated from the flask. The cell side of the flask was washed with 4 ml of trypsin which was allowed to spread across the entire surface for around a minute (was left long enough for the cells to detach from the inside of the flask). 6 ml of media was used to wash the cell side of the flask to inactivate the trypsin, and a serological pipette was used to rinse this mixture of media, trypsin, and cells multiple times to collect all the cells at the bottom of the flask. This mixture was placed into a 15 ml falcon tube and centrifuged for 5 minutes at 1500 rpm, 4°C.

The media was aspirated from the tube leaving the pellet of cells at the bottom which was resuspended in 3 ml of media. Two new cell culture flasks were used for the splitting process (in addition to the original flask used earlier), and 1 ml of the resuspended cells mixed with media was placed into each of the three cell culture flasks. 19 ml of media was added to each of the flasks, resulting in three flasks that each had 20 ml of media. The flasks were placed in a 37°C incubator for 2-3 days, and this process of splitting cells was repeated based on cell confluency (around every 2-3 days) until 9 viable flasks of cells were made.

Viral Transfection with Lipofectamine 3000

When cells reached a confluency level of around 70-80%, they were ready to be used for this transfection process. The day before the transfection, the cells were detached from the cell culture flasks and replated into multiple 6-well plates, and each well had between $0.5\text{-}2*10^5$ adherent cells in them. 0.75 and 1.5 µl of Lipofectamine 3000 Reagent were diluted in two separate tubes that had 25 µl of Opti-MEM Medium by putting the tubes in a vortex mixer for 3 seconds. 1 µg of DNA was put into a new tube, which was filled with 50 µl of Opti-MEM Medium to prepare the plasmid DNA. 2 µl of P3000 Reagent was added to the new tube which was vortexed to dilute the contents, and the diluted DNA mixture was added to each tube of the diluted Lipofectamine 3000 reagent at an equal 1:1 ratio. The tubes were incubated for 10 minutes at room temperature, and after this time, 50 µl of the DNA-lipid complex was added to the cells which were incubated at 37°C for 2-4 days, after which time the supernatant (containing the newly generated virus secreted from the transfected cells) was collected and frozen for storage to be used later in the experiment.

Viral Transfection with PEI

When cells reached a confluency level of around 60-70%, they were ready to be used for this transfection process. 30 µl of media were placed in a sterile tube with an added 0.5 µg of DNA and an additional 1.5 µg of PEI for each well (based on a 6-well plate) to maintain a 3:1 ratio. A negative control was made by adding 9 µg of PEI to 200 µl of media (without the plasmid DNA) and the tubes were incubated at room temperature for 15 minutes. This mixture was added to each well of cells in a 3:1 volume to cells ratio and the cells were incubated with this DNA/PEI mixture for 4 hours at 37°C. The media containing the DNA/PEI mixture was removed and replaced with 2-3 ml of fresh media. The plates were incubated for 1-2 days at 37°C to allow for plasmid expression, after which time the supernatant was collected and frozen for storage to be used later in the experiment.

Isolation of Peripheral Blood Mononuclear Cells (PBMCs) from Healthy Human Blood

A trained phlebotomist drew between 120-180 ml of blood from healthy donors in accordance with University of Utah Institutional Review Board (IRB) Protocol 67637 using a 60 ml syringe containing 5 ml of anticoagulant. 15 ml of Lymphoprep was placed into two 50 ml falcon tubes per syringe of blood, and the blood was slowly layered over the Lymphoprep by tilting the tube (in order to not let the two layers mix). The blood from the syringes was divided equally between two tubes so that they would balance each other in the centrifuge. This layering step was repeated for the other tubes which were then centrifuged for 30 minutes at 1400 rpm, 4°C (the acceleration and deceleration were set at 0 so that the layers weren't disturbed), to separate the buffy coat (containing the PBMCs) from the red blood cells. A 10 ml pipette was used to harvest the lower cloudy layer which contains PBMCs, and these cells were washed twice with the PBS.

Isolation of the Cluster of Differentiation 14 (CD14+) Monocytes

The PBMCs were incubated with Milteny microbeads coated with CD14 antibody and Milteny MACs buffer for 30 minutes at 4°C. 10 ml of MACs buffer was added and the beads and cells were centrifuged for 5 minutes at 1500 rpm, 4°C. A Milteny MACs column and an appropriate magnet were used to wet the column with 3 ml of MACs buffer. The MACs buffer was aspirated out of centrifuged tube, leaving a pellet of cells and beads, which was resuspended in 1 ml of MACs buffer. The resuspended cells and beads were pipetted into the MACs column and passed through until no more drips exited the column. The column was washed 3 times with 3 ml of MACs buffer, taking care to wait for drips to stop exiting the column between washes. 5 ml of media was put into an unused sterile 15 ml falcon tube, and after the dripping from column stopped following the third wash, the column from the magnet was removed and placed onto the top of the new 15 ml falcon tube. 5 ml of MACs buffer was pipetted into the top of the column and a plunger was used to quickly force the MACs buffer through the column (this washed the cells and beads that were held in the column by the magnet out of the column and into the 15 mL falcon tube). The media containing the pure population of CD14+ monocytes was centrifuged for 5 minutes at 1500 rpm, 4°C, and was then resuspened at 1 million cells per ml of serum free media. 600 µl of cells (totaling 600,000 cells) were pipetted into the required number of wells of 24-well plates until all cells were plated, and the plates were put in a 37°C incubator for 2 hours, to allow monocytes to adhere to the bottom of the wells. After the cells adhered, the media was removed and replaced with complete RPMI media containing 9% FBS and 9% pooled human serum in addition to the L-glutamine as described earlier in this methods section.

These monocytes were incubated at 37°C for 5 days to allow them to differentiate into monocyte derived macrophages (MDMs). On the 6^{th} day, the media was changed and they were placed back in the incubator at 37°C. On the 7^{th} day, the cells could be used for experimental purposes.

Primary and Secondary Infection of Macrophages.

The frozen virus was thawed appropriate varying amounts was put in each of the wells containing MDMs for the first infection. On the 8^{th} day, additional virus was thawed and appropriate varying amounts were put in each of the wells containing MDMs for the second infection. The media was changed on both the 9^{th} and 10^{th} days.

Flow Cytometry

MDMs were detached by washing each well with 500 µl of PBS, and replacing with 200 µl of Accutase, and incubating at 37°C for a minimum of two hours. The cells were transferred

to appropriately labeled flow cytometry tubes and 1 ml of PBS was added to each tube and centrifuged for 5 minutes at 1500 rpm, 4°C. The PBS was aspirated and cells were stained with a viability dye (Bioscience Fixable Viability Dye eFluor 450), using 0.4 µl of dye per tube, and incubated for 30 minutes at 4°C. Cells were measured using flow cytometry (Attune NxT Flow Cytometer from Thermo Fisher) to assess their viability, as well as their level of infection (based on their fluorescence intensity).

RESULTS

Proof of Bystander Effect and Development of Hypothesis

The initial experiments in our lab that lead to our hypothesis are visualized in figure 6. This experiment paired an initial HIV infection with a constant level of a secondary infection, to determine if a protective response is seen (Fig. 6). The primary infection was done using a dHIV-mCherry virus, making infected cells appear red. The second infection was done with a dHIV-gfp virus, which would turn infected cells green. This experiment showed that an initial infection with HIV is able to offer increasing degrees of protection from a secondary infection of HIV depending on how much virus was used during the first infection (Szaniawski, unpublished). A small initial infection was able to show sizable protection, and a large initial infection was able to offer near complete protection from the secondary infection (Fig. 6b).

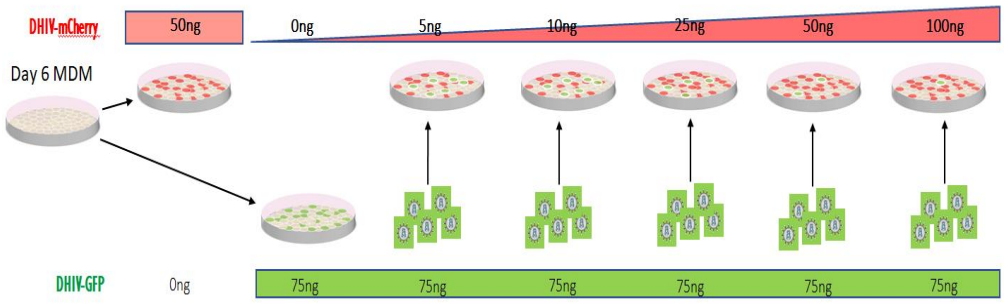

6a.

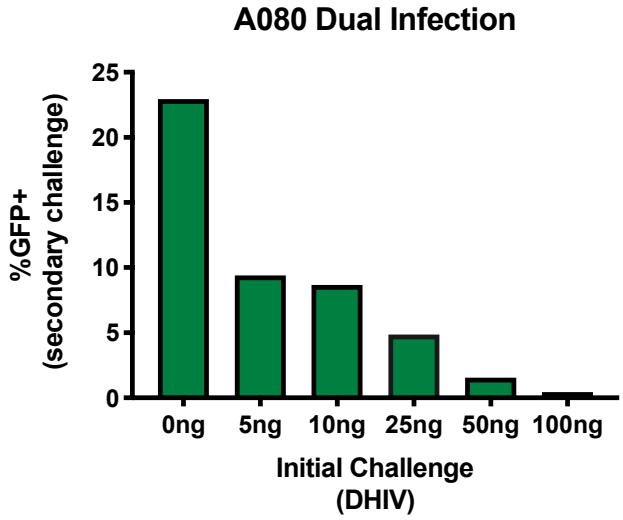

b.

Fig. 6. a. A graphical representation of the experiment structure that proved the bystander effect to be real. The initial infection used dHIV-mCherry virus with increasing levels of infection, while the secondary infection used a constant level of dHIV-gfp virus. b. The results of the experiment proved the bystander effect to be real based on higher levels of cell protection in relation to higher initial infections. (Credit to: Elizabeth Williams & Matt Szaniawski, Unpublished data).

After observing the bystander effect, the question that I addressed with my research is, "What is causing the bystander effect to occur?" To answer this question, we repeated some of the initial experiments, and expanded upon them using additional techniques and more pseudotyped viruses.

As explained in the introduction, MDMs infected with a VSVg-dHIV virus induced a stronger degree of SAMHD1 dephosphorylation and protection from secondary infection than the replication competent virus (Fig. 5). In theory, the viral envelope is the only difference between these two viruses. This led us to think that the viral envelope is responsible for inducing the bystander effect and we based our experiments around this hypothesis. Since we wanted the viral envelope to be the only changing variable in this study, we pseudotyped the HIV viral core with the envelopes of other viruses. Through these experiments, we were able to see changes in the level of secondary infection.

Experimental Design Development: Establishment of Flow Cytometry Controls

Flow cytometry is a tool used to quantify populations based on specific properties. The properties that you choose to assess can be then stained with a fluorescent dye, and you can stain for multiple properties at the same time with different colours of fluorescent dyes. The cells are linearized into a single cell stream in the flow cytometer, passed through a chamber where multiple lasers shine on them, and the dyes emit fluorescence when a specific laser that excites that dye can be counted. This is then quantified into a number describing the amount of each specific property stained for in the experiment. Additionally, there are molecular tools that we can use to "tag" cellular proteins with fluorescent dyes. For example, if we infect a cell with a dHIV-gfp pseudotyped virus, when the cell generates viral proteins, it will fluoresce green allowing the flow cytometer to count the cells as "infected".

In order for flow data to be used for experimental measurements, we must first establish controls. To do this, we used cells that were infected with a dHIV-mCherry virus, which while infected, would make cells fluoresce red when hit with the appropriate laser (Figure 7). Panel 6a shows the area in the rectangle used to establish a "gate". The X axis on the graph shows number of dHIV-gfp positive cells- those toward the origin are negative, while those within the box are positive for gfp. The gate was established by measuring gfp fluorescence in cells infected with a dHIV-mCherry virus, thus establishing a population that is "negative" (those that are to the left of the rectangle) and establishing what will be "positive" (those inside the rectangle). As expected, when we apply the gate to samples that should show gfp positive cells positive cells are observed in abundance in the rectangle (figure 7b). We were also interested in identifying cells that have been infected by both the virus that fluoresces green (dHIV-gfp) and the virus that fluoresces red (mCherry). In figure 7c dHIV-gfp is on the X axis, but the Y axis depicts dHIV-mCherry, and no mCherry positive cells are detected, which is expected if the cells were only infected with a virus that encoded gfp.

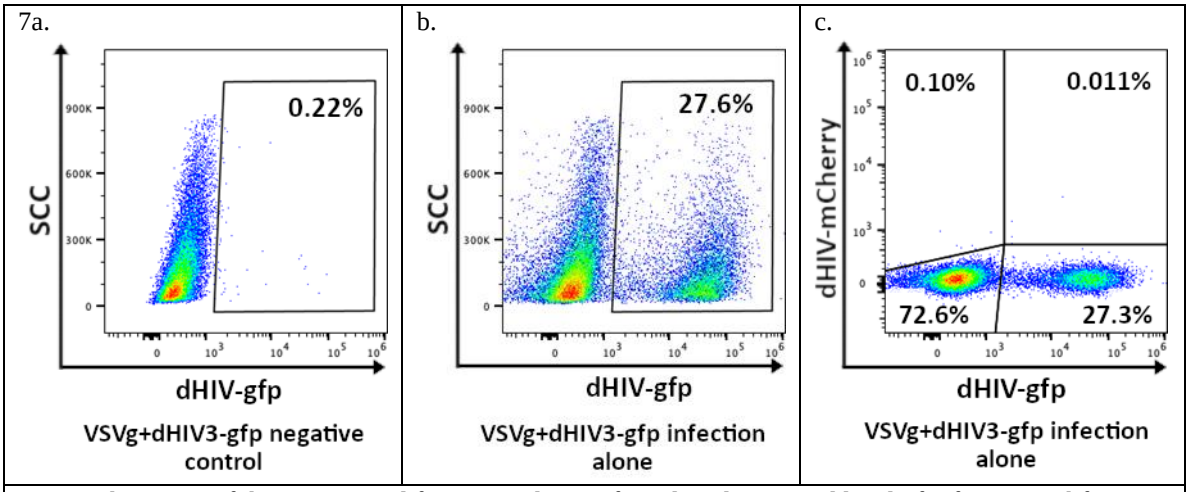

Fig. 7. The set-up of the gate control for VSVg-dHIV-gfp and its determined level of infection. Subfigure a. shows a 0.22% level of infection, and using the same gate, Subfigure b. shows a 27.6% level of infection. Subfigure c. combines the gates from the previous subfigures.

We established the same negative controls for the dHIV-mCherry viruses (Fig. 8a). This gate acted as a negative control and was then used to determine the level of infection for all of our viruses that had the dHIV-mCherry core (Fig. 8b & 7c).

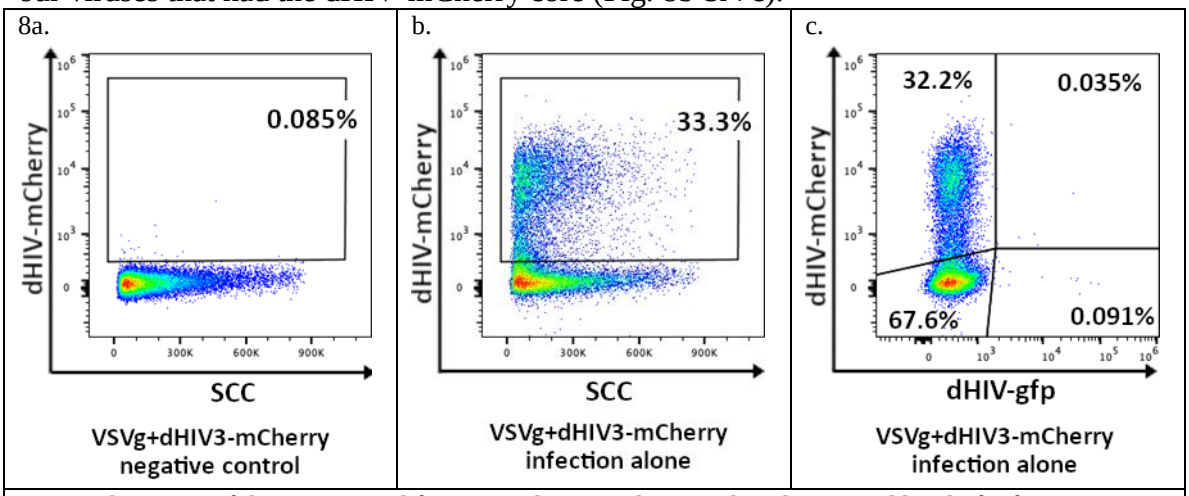

Fig. 8. The set-up of the gate control for VSVg-dHIV-mCherry and its determined level of infection. Subfigure a. shows a 0.085% level of infection, and using the same gate, Subfigure b. shows a 33.3% level of infection. Subfigure c. combines the gates from the previous subfigures.

VSVg pseudotyped virus infected cells show strong bystander effect

Once the controls were established, we used them to study the cells that experienced a primary infection with VSVg+dHIV3-gfp and a secondary infection of VSVg+dHIV3-mCherry. The primary infection showed the gfp cells with an infection level of 39.7% (Fig. 9a). The secondary infection showed the mCherry cells with an infection level of 6.67% (Fig. 9b). When we look at both gfp and mCherry together in Figure 9c, the cells infected with the VSVg-dHIV-gfp virus (first infection; shown in the right two quadrants of the graph) 34.9% + 4.46% = 39.36% of cells were infected in the first infection. The cells that were infected with the VSVg-dHIV-mCherry virus (second infection) are shown in the top two quadrants of the graph (1.27% + 4.46% = 5.73% of cells were infected in the second infection). So when we compare the amount of single infection from the VSVg-dHIV-gfp virus that we have as a control in figure 7b (27.6%) to the first infection in figure 9c (39.36%), we see that the two single infections are

similar to each other. When we compare the amount of single infection from the VSVg-dHIV-mCherry virus that we have as a control in figure 8b (33.3%) to the secondary infection level in figure 9c (5.73%), you can see that there is a bystander response following the first infection, which induces protection in these cells from the second infection: 33.3% drops to 5.73%, a 5.8-fold reduction in the amount of infection. Interestingly, of the cells that are infected by the second infection (5.73%), almost all of them (77.8%) were infected by the VSVg-dHIV-gfp virus during the first round of infection. This further shows that the bystander effect is occurring in the cells that were not infected in the first round of infection: 39.36% of cells were infected in the first infection, of those 11.3% were reinfected by the second infection, which is compared to the 60.67% that were uninfected after the first round of infection, of those, only 2.1% were infected in the second infection. In conclusion, the bystander cells were 5.38-fold less likely to be infected than the cells that were infected in the first round of infection.

9a.

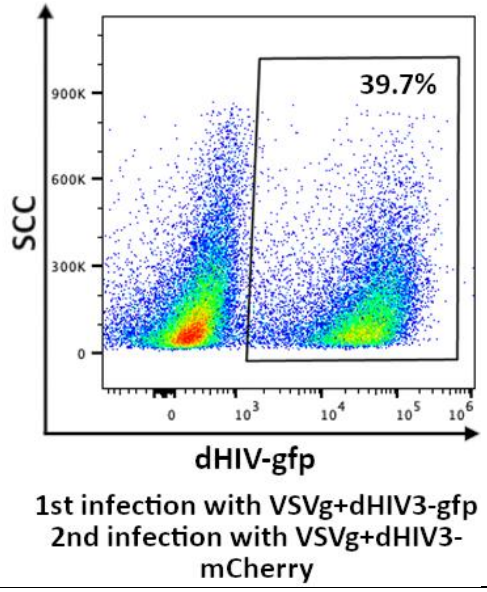

b.

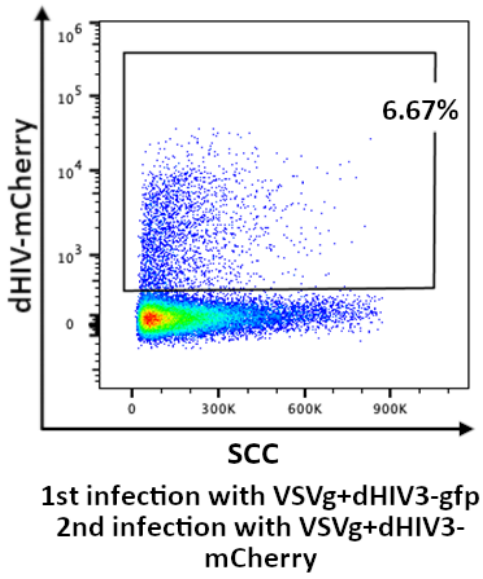

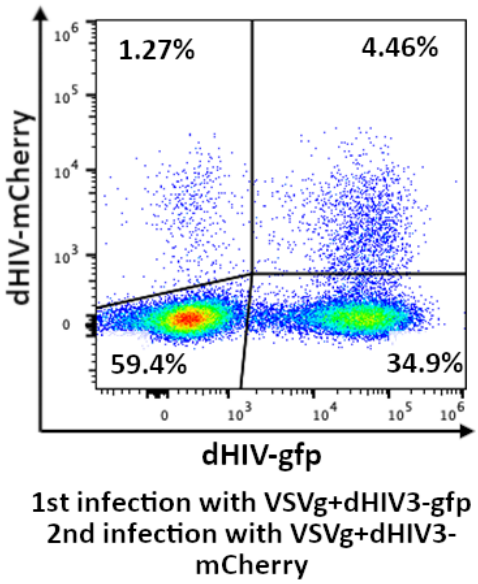

c.

Fig. 9. The determined level of infection with a primary infection of VSVg-dHIV3-gfp and secondary infection of VSVg-dHIV3-mCherry. Subfigure a. shows a 39.7% infection for the GFP cells while Subfigure b. shows a 6.67% level of infection. Subfigure c. combines the gates from the previous subfigures.

Bystander effect in VSVg pseudotyped virus for first infection, AMLV pseudotyped virus for second infection

Using the same gates that were established in the first example, we can assess the single infection baseline for the viruses that we pseudotyped with other viral envelopes. Figure 10b shows that the single infection with the AMLV pseudotyped virus (AMLV-dHIV-mCherry) achieved an infection of 5.89% of cells. But when you use the AMLV-dHIV-mCherry virus as the secondary virus (the first virus remains the VSVg-dHIV-gfp pseudotyped virus, infection level 36.72%), the percentage of cells infected is only 0.12% (Fig. 11b). Again, we can compare this result to the single AMLV-dHIV-mCherry infection (5.89% to 0.12%, a 50-fold reduction). We can also compare the percentage of cells infected by the first virus that were then infected by the second virus (0.05%), to the percentage of cells that were not infected during the first round of infection, but were able to be infected in the second infection (0.14%). From this we see that the VSVg-dHIV-gfp infection completely protected both the infected cells and the uninfected cells from a second round of infection.

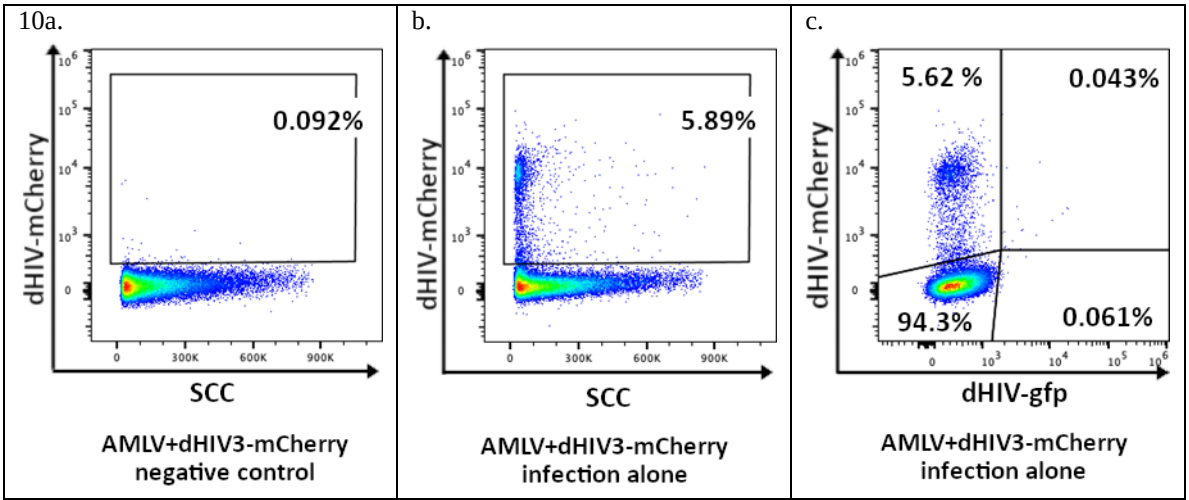

Fig. 10. The set-up of the gate control for AMLV-dHIV-mCherry and its determined level of infection. Subfigure a. shows a 0.092% level of infection, and using the same gate, Subfigure b. shows a 5.89% level of infection. Subfigure c. combines the gates from the previous subfigures.

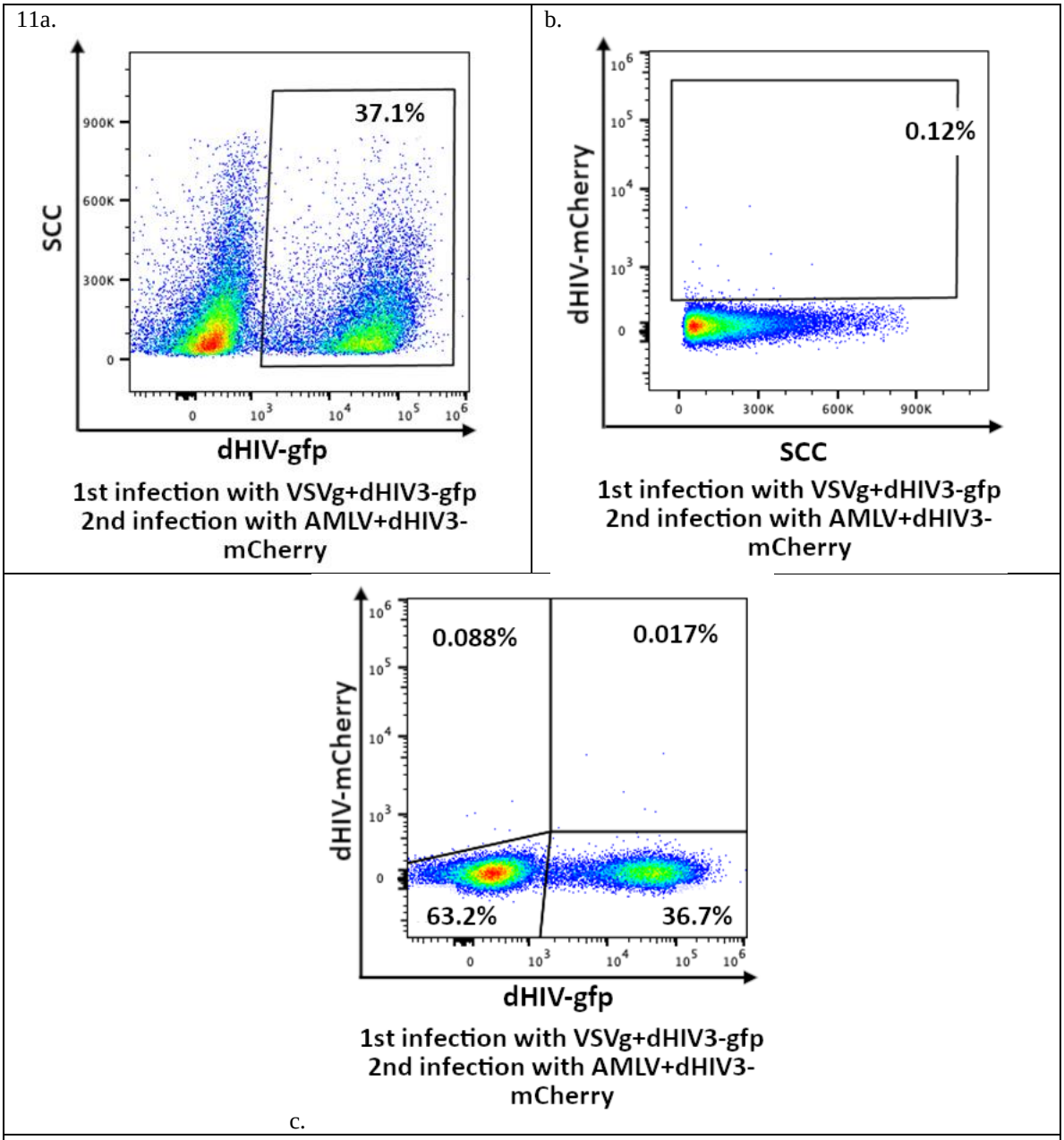

Fig. 11. The determined level of infection with a primary infection of VSVg-dHIV3-gfp and secondary infection of AMLV-dHIV3-mCherry. Subfigure a. shows a 37.1% infection for the GFP cells while Subfigure b. shows a 0.12% level of infection. Subfigure c. combines the gates from the previous subfigures.

AMLV pseudotyped viruses for both first and second rounds of infection

When the first round of infection is conducted with an AMLV-dHIV-gfp pseudotyped virus, we have an initial level of infection of 4.13% (Fig. 13a). When we do a single round of infection with the AMLV-dHIV-mCherry virus we see an infection level of 5.89% (Fig. 10b). When we use the AMLV-dHIV-mCherry virus for the second round of infection, we see that only 1.89% of cells are infected, which is a 3.12-fold decrease in infection. When we compare the percentage of cells that were infected by the first virus, and were also infected by the second virus (8.37%), to the percentage of cells that were not infected by the first virus, but were infected by the second virus (1.5%), we see that the bystander effect is occurring more

significantly in the uninfected cells than in those that were infected by AMLV-dHIV-gfp in the first round of infection.

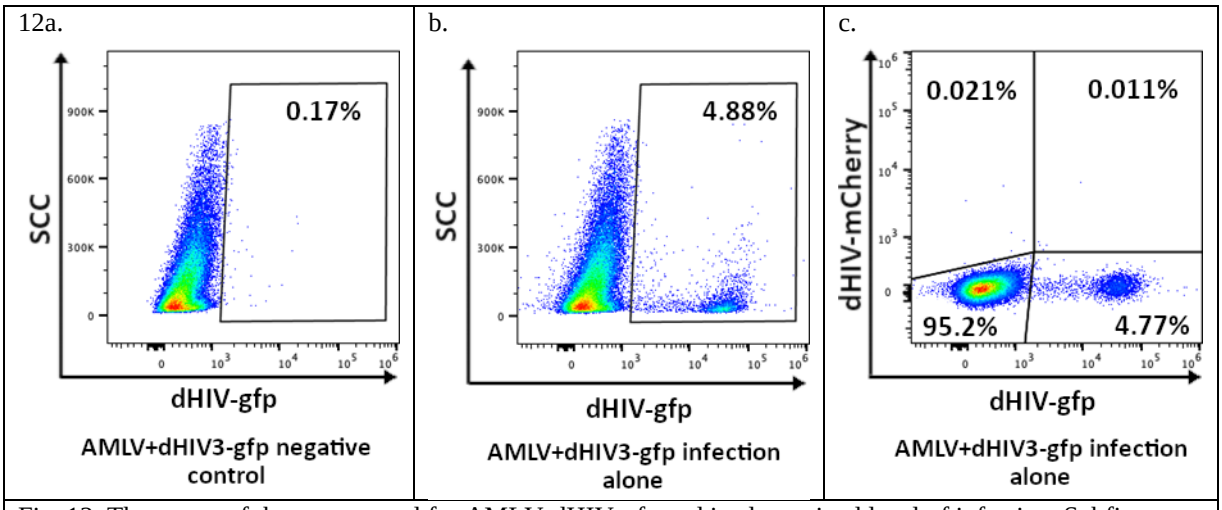

Fig. 12. The set-up of the gate control for AMLV-dHIV-gfp and its determined level of infection. Subfigure a. shows a 0.17% level of infection, and using the same gate, Subfigure b. shows a 4.88% level of infection. Subfigure c. combines the gates from the previous subfigures.

AMLV pseudotyped virus for the first round of infection, VSVg pseudotyped virus for the second round of infection

The first round of infection with the AMLV-dHIV-gfp virus infected 2.24% of cells (Fig. 14a). When the VSVg-dHIV-mCherry virus is used as a single infection, it reaches an infection level of 33.3% (Fig. 8b). When we use the VSVg-dHIV-mCherry virus for the second infection after a primary infection by AMLV-dHIV-gfp (as opposed to a primary infection with the VSVg pseudotyped virus), we see an infection level of 19.67% figure 14c, which is a 1.7-fold change from the VSVg-dHIV-mCherry virus in a single infection. When we compare the percentage of cells that were infected in the first round of infection that were also infected in the second round of infection (40.2%), to the percentage of cells that were uninfected by the first round of infection that were infected in the second round of infection (23.8%), we again see the same lack of protection in both the infected and uninfected cells.

13a.

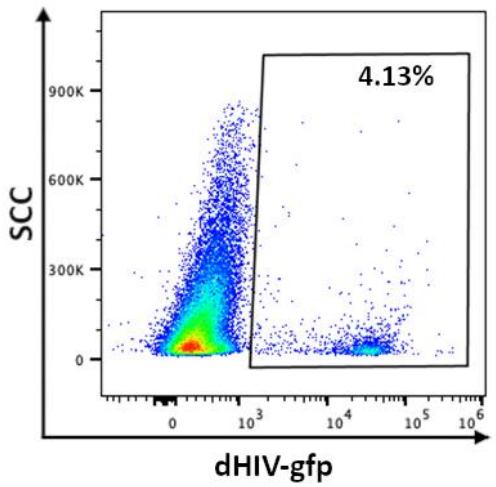

1st infection with AMLV+dHIV3-gfp
2nd infection with AMLV+dHIV3-mCherry

b.

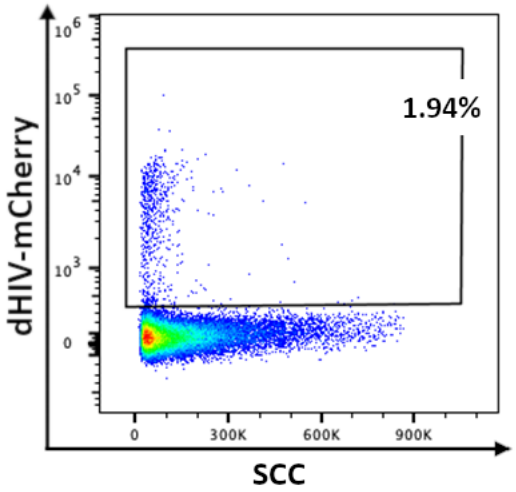

1st infection with AMLV+dHIV3-gfp
2nd infection with AMLV+dHIV3-mCherry

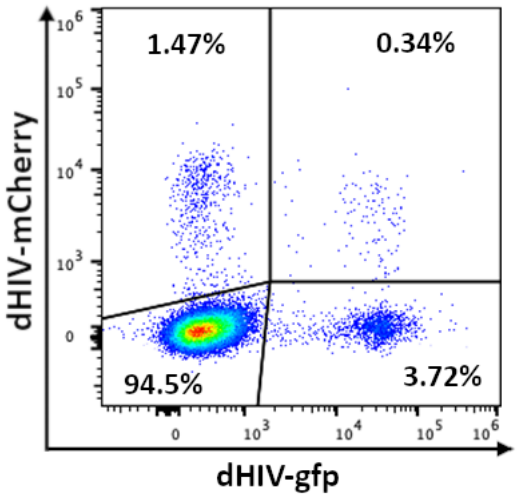

1st infection with AMLV+dHIV3-gfp
2nd infection with AMLV+dHIV3-mCherry

c.

Fig. 13. The determined level of infection with a primary infection of AMLV-dHIV3-gfp and secondary infection of AMLV-dHIV3-mCherry. Subfigure a. shows a 4.13% infection for the GFP cells while Subfigure b. shows a 1.94% level of infection. Subfigure c. combines the gates from the previous subfigures.

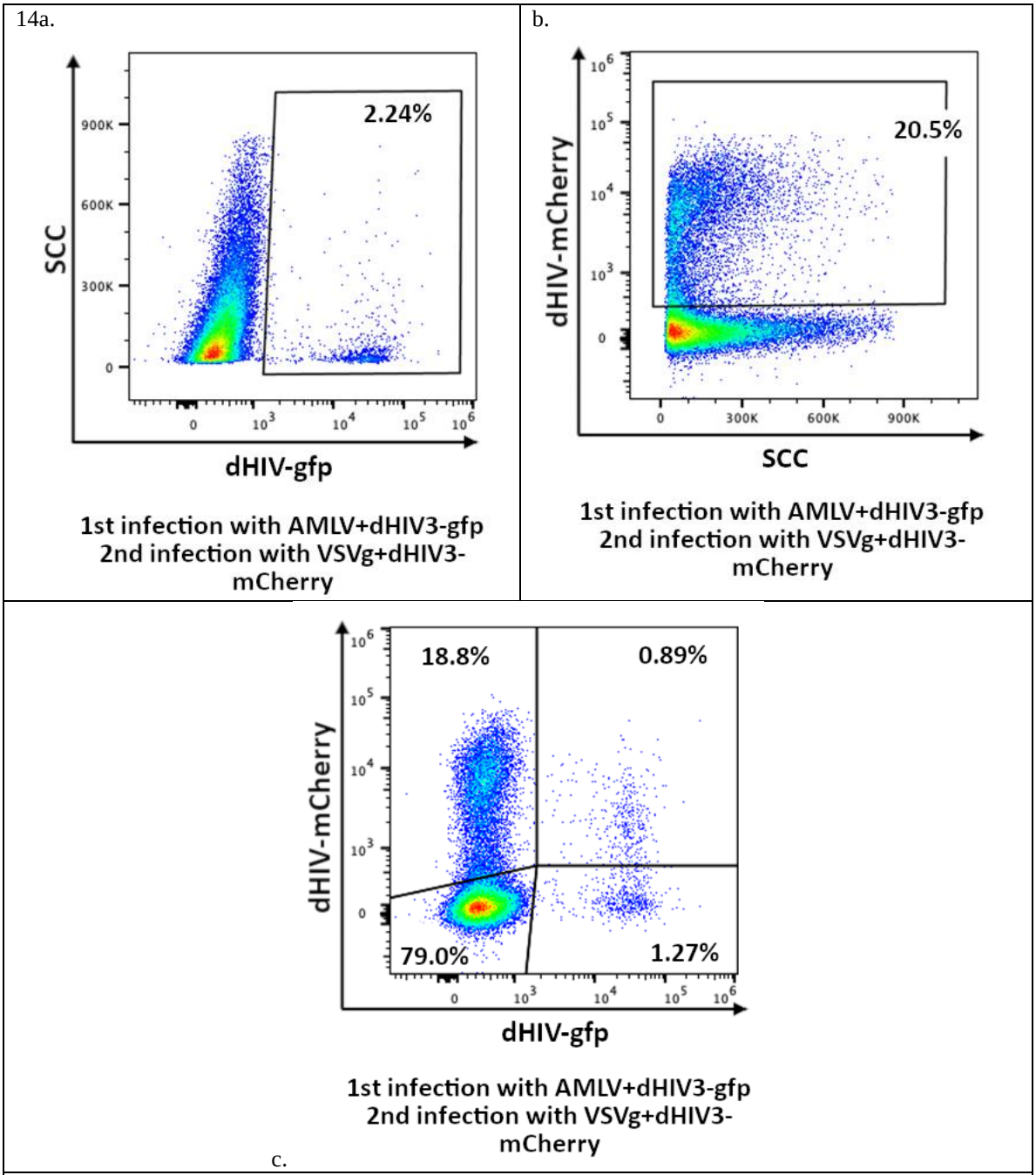

Fig. 14. The determined level of infection with a primary infection of AMLV-dHIV3-gfp and secondary infection of VSVg-dHIV3-mCherry. Subfigure a. shows a 2.24% infection for the GFP cells while Subfigure b. shows a 20.5% level of infection. Subfigure c. combines the gates from the previous subfigures.

The flow cytometry data is summarized in a table with all the combinations of first and second infections that were conducted. The cells coloured grey did not have a substantial initial infection which made those infections insignificant. VSVg, AMLV, and LCMV all showed significant levels of initial infection when exposed to gfp (single column under 1st GFP) or mCherry (single row right of 2nd mCherry), which is why their data was considered viable (Fig. 15).

An initial infection of VSVg (41.7%) paired with a secondary infection of VSVg produced a 6.67% level of infection. An initial infection of VSVg was paired with a secondary

infection of AMLV produced a 0.12% level of infection. An initial infection of VSVg paired with a secondary infection of LCMV produced a 0.14% level of infection. An initial infection of AMLV (4.88%) paired with a secondary infection of VSVg produced a 20.5% level of infection. An initial infection of AMLV paired with a secondary infection of AMLV produced a 1.94% level of infection. An initial infection of AMLV paired with a secondary infection of LCMV produced a 0.98% level of infection. An initial infection of LCMV (5.2%) paired with a secondary infection of VSVg produced a 30.8% level of infection. An initial infection of LCMV paired with a secondary infection of AMLV produced a 4.58% level of infection. An initial infection of LCMV paired with a secondary infection of LCMV produced a 1.64% level of infection (Fig. 15).

		JRFL	VSVg	AMLV	GMTR	Lassa	RD114	LCMV
	1st (GFP) ↓ 2nd (mCherry)→	0.21	33.4	5.89	0.49	0.11	0.15	2.56
JRFL	0.44	0.17	17.6	2.73	0.21	0.082	0.14	1.86
VSVg	41.7	0.1	6.67	0.12	0.098	0.067	0.13	0.14
AMLV	4.88	0.21	20.5	1.94	0.16	0.099	0.11	0.98
GMTR	0.14	0.12	18.4	2.61	0.2	0.052	0.11	2.18
Lassa	0.22	0.19	24.9	5.23	0.35	0.1	0.12	1.52
RD114	0.32	0.19	33.4	5.88	0.29	0.045	0.14	1.61
LCMV	5.2	0.17	30.8	4.58	0.49	0.072	0.15	1.64

Fig. 15. A complete summary of all the data collected from the flow cytometry plots. The first column indicates the level of infection of only a single infection with GFP as the fluorescent protein, and the first row indicates the level of infection of only a single infection with mCherry as the fluorescent protein.

DISCUSSION

The results presented in this thesis show a clear shift in cell infection levels when the viral envelope was changed. The viral envelopes of VSVg, AMLV, and LCMV all showed some degree of bystander effect related relationship. It was surprising to see protection levels from infection at 99% or greater in some of these primary infections paired with secondary infections. Clear examples of this were seen in the primary infection of VSVg paired with the secondary infection of AMLV or LCMV, as well as the primary infection of AMLV paired with the secondary infection of LCMV. Other clear examples of the bystander effect were seen in the primary infection of VSVg paired with the secondary infection of VSVg, AMLV paired with the secondary infection of AMLV, as well as the primary infection of LCMV paired with the secondary infections of either AMLV or LCMV (Fig. 15). All of these results extended the research related to the original bystander effect experiments from the Planelles lab.

The data that seemed to be the most confusing was related to the viral envelopes that each experienced the secondary infection of VSVg. All of the primary infections that had a secondary infection of VSVg (with an exception to the primary infection of VSVg) had significantly less

protection compared to the other viral envelopes in Fig. 15. Even though we don't know why the secondary infection of VSVg was giving so little protection, it was a unique trend to take note of and could be an interesting vein of research to later pursue.

An important limitation in our research model relates to the highly varying levels of initial infection present in our experiments. The single initial infection of GFP had infection levels of 41.7%, 4.88%, and 5.2% with the viral envelopes of VSVg, AMLV, and LCMV respectively. These varying levels could also be seen in the single initial infection of mCherry at infection levels of 33.4%, 5.89%, and 2.56% with the viral envelopes of VSVg, AMLV, and LCMV respectively (Fig. 15). Finding a way to control for these values is necessary to create comparable situations to better understand the bystander effect. The higher initial infection of VSVg in both GFP and mCherry could potentially be the reason the secondary infection viral envelopes of VSVg seemed to offer lower levels of protection compared to the other viral envelopes. Even though the percentage of cells protected was lower in VSVg, the number of total cells protected is significantly higher due to the higher initial infection level. This understanding makes the results with the primary viral envelope of VSVg especially interesting, as they had some of the highest levels of protection offered (Fig. 15).

Another potential variable that we were unable to test, but might be important to look at, is the change in bystander effect if the HIV core was changed rather than the viral envelope. Based on the current literature, we believe that changing the core will not have an effect, but creating an experiment to test this would confirm this hypothesis. We plan to test this by looking at infection levels between two different cores of dHIV and MLV, and if there is no significant difference in infection levels, we could state the core likely isn't impacting the bystander effect.

The future of this project will explicitly be looking at the role of IFITM3 in the protection offered by the bystander effect. We predict that the bystander effect could potentially be caused partially, if not entirely, by this protein. This hypothesis will be tested by removing IFITM3 from cells, and comparing the levels of the bystander effect to control cells. By using neon electroporation and CRISPR technology, we will genetically knockout IFITM3 to see if this hypothesis is true. We hope these future experiments will inform us of the exact cause of the bystander effect, allowing for new experiments and potential therapeutic techniques to be developed.

REFERENCES

Damtie, D., Yismaw, G., Woldeyohannes, D., & Anagaw, B. (2013). Common opportunistic infections and their CD4 cell correlates among HIV-infected patients attending at antiretroviral therapy clinic of Gondar University Hospital, Northwest Ethiopia. *BMC research notes, 6*, 534. https://doi.org/10.1186/1756-0500-6-534

Lloyd A. (1996). HIV infection and AIDS. *Papua and New Guinea medical journal, 39*(3), 174–180.

Gayle, H. D., & Hill, G. L. (2001). Global impact of human immunodeficiency virus and AIDS. *Clinical microbiology reviews, 14*(2), 327–335. https://doi.org/10.1128/CMR.14.2.327-335.2001

Montessori, V., Press, N., Harris, M., Akagi, L., & Montaner, J. S. (2004). Adverse effects of antiretroviral therapy for HIV infection. *CMAJ : Canadian Medical Association journal = journal de l'Association medicale canadienne, 170*(2), 229–238.

Wong, M. E., Jaworowski, A., & Hearps, A. C. (2019). The HIV Reservoir in Monocytes and Macrophages. *Frontiers in immunology, 10*, 1435. https://doi.org/10.3389/fimmu.2019.01435

Deeks, S. G., Overbaugh, J., Phillips, A., & Buchbinder, S. (2015). HIV infection. *Nature reviews. Disease primers, 1*, 15035. https://doi.org/10.1038/nrdp.2015.35

Rossi, E., Meuser, M. E., Cunanan, C. J., & Cocklin, S. (2021). Structure, Function, and Interactions of the HIV-1 Capsid Protein. *Life (Basel, Switzerland), 11*(2), 100. https://doi.org/10.3390/life11020100

De Clercq E. (2010). Antiretroviral drugs. *Current opinion in pharmacology, 10*(5), 507–515. https://doi.org/10.1016/j.coph.2010.04.011

Leech, A. A., Biancarelli, D., Aaron, E., Miller, E. S., Coleman, J. S., Anderson, P. L., Nkwihoreze, H., Condron, B., & Sullivan, M. (2020). HIV Pre-Exposure Prophylaxis for Conception Among HIV Serodiscordant Couples in the United States: A Cohort Study. *AIDS patient care and STDs, 34*(7), 295–302. https://doi.org/10.1089/apc.2020.0005

Mahy, M., Marsh, K., Sabin, K., Wanyeki, I., Daher, J., & Ghys, P. D. (2019). HIV estimates through 2018: data for decision-making. *AIDS (London, England), 33 Suppl 3*(Suppl 3), S203–S211. https://doi.org/10.1097/QAD.0000000000002321

Wirth, T., Parker, N., & Ylä-Herttuala, S. (2013). History of gene therapy. *Gene, 525*(2), 162–169. https://doi.org/10.1016/j.gene.2013.03.137

Buchschacher, G. L., Jr, & Wong-Staal, F. (2000). Development of lentiviral vectors for gene therapy for human diseases. *Blood, 95*(8), 2499–2504.

Pluta, K., & Kacprzak, M. M. (2009). Use of HIV as a gene transfer vector. *Acta biochimica Polonica, 56*(4), 531–595.

Colomer-Lluch, M., Ruiz, A., Moris, A., & Prado, J. G. (2018). Restriction Factors: From Intrinsic Viral Restriction to Shaping Cellular Immunity Against HIV-1. *Frontiers in immunology, 9*, 2876. https://doi.org/10.3389/fimmu.2018.02876

Cribier, A., Descours, B., Valadão, A. L., Laguette, N., & Benkirane, M. (2013). Phosphorylation of SAMHD1 by cyclin A2/CDK1 regulates its restriction activity toward HIV-1. *Cell reports, 3*(4), 1036–1043. https://doi.org/10.1016/j.celrep.2013.03.017

Coggins, S. A., Mahboubi, B., Schinazi, R. F., & Kim, B. (2020). SAMHD1 Functions and Human Diseases. *Viruses, 12*(4), 382. https://doi.org/10.3390/v12040382

Compton, A. A., Roy, N., Porrot, F., Billet, A., Casartelli, N., Yount, J. S., Liang, C., & Schwartz, O. (2016). Natural mutations in IFITM3 modulate post-translational regulation and toggle antiviral specificity. *EMBO reports, 17*(11), 1657–1671. https://doi.org/10.15252/embr.201642771

Miletic, H., Bruns, M., Tsiakas, K., Vogt, B., Rezai, R., Baum, C., Kühlke, K., Cosset, F. L., Ostertag, W., Lother, H., & von Laer, D. (1999). Retroviral vectors pseudotyped with lymphocytic choriomeningitis virus. *Journal of virology, 73*(7), 6114–6116. https://doi.org/10.1128/JVI.73.7.6114-6116.1999

Bentley, E. M., Mather, S. T., & Temperton, N. J. (2015). The use of pseudotypes to study viruses, virus sero-epidemiology and vaccination. *Vaccine, 33*(26), 2955–2962. https://doi.org/10.1016/j.vaccine.2015.04.071

Landau, N. R., & Littman, D. R. (1992). Packaging system for rapid production of murine leukemia virus vectors with variable tropism. *Journal of virology, 66*(8), 5110–5113. https://doi.org/10.1128/JVI.66.8.5110-5113.1992

Tandon, R., Mitra, D., Sharma, P. et al. Effective screening of SARS-CoV-2 neutralizing antibodies in patient serum using lentivirus particles pseudotyped with SARS-CoV-2

spike glycoprotein. *Sci Rep 10*, 19076 (2020). https://doi.org/10.1038/s41598-020-76135-w

Kim, TS., Shin, EC. The activation of bystander CD8+ T cells and their roles in viral infection. *Exp Mol Med 51*, 1–9 (2019). https://doi.org/10.1038/s12276-019-0316-1

Garg, H., & Joshi, A. (2017). Host and Viral Factors in HIV-Mediated Bystander Apoptosis. *Viruses, 9*(8), 237. https://doi.org/10.3390/v9080237

DePolo, N. J., Reed, J. D., Sheridan, P. L., Townsend, K., Sauter, S. L., Jolly, D. J., & Dubensky, T. W., Jr (2000). VSV-G pseudotyped lentiviral vector particles produced in human cells are inactivated by human serum. *Molecular Therapy : The Journal of the American Society of Gene Therapy, 2*(3), 218–222. https://doi.org/10.1006/mthe.2000.0116

Szaniawski, M. A., Spivak, A. M., Cox, J. E., Catrow, J. L., Hanley, T., Williams, E., Tremblay, M. J., Bosque, A., & Planelles, V. (2018). SAMHD1 Phosphorylation Coordinates the Anti-HIV-1 Response by Diverse Interferons and Tyrosine Kinase Inhibition. *mBio, 9*(3), e00819-18. https://doi.org/10.1128/mBio.00819-18